Comput Mech (2008) 41:707–714
DOI 10.1007/s00466-007-0226-2

ORIGINAL PAPER

Stochastic Finite element analysis of the free vibration of functionally graded material plates

Afeefa Shaker · Wael Abdelrahman · Mohammad Tawfik · Edward Sadek

Received: 28 August 2007 / Accepted: 3 November 2007 / Published online: 8 January 2008

Abstract The superior properties of functionally graded materials (FGM) are usually accompanied by randomness in their properties due to difficulties in tailoring the gradients during manufacturing processes. Using the stochastic finite element method (SFEM) proved to be a powerful tool in studying the sensitivity of the static response of FGM plates to uncertainties in their material properties. This tool is yet to be used in studying free vibration of FGM plates. The aim of this work is to use both a First Order Reliability Method (FORM) and the Second Order Reliability Method (SORM), combined with a nine-noded isoparametric Lagrangian element based on the third order shear deformation theory to investigate sensitivity of the fundamental frequency of FGM plates to material uncertainties. These include the effect of uncertainties on both the metal and ceramic constituents. The basic random variables include ceramic and metal Young's modulus and Poisson's ratio, their densities and ceramic volume fraction. The developed code utilizes MATLAB capabilities to derive the derivatives of the stiffness and mass matrices symbolically with a considerable reduction in calculation time. Calculating the eigenvectors at the mean values of the variables proves to be a reasonable simplification which significantly increases solution speed. The stochastic finite element code is validated using available data in the literature, in addition to comparisons with results of the well-established Monte Carlo simulation technique with importance sampling. Results show that SORM is an excellent rapid tool in the stochastic analysis of free vibration of FGM plates, when compared to the slower Monte Carlo simulation techniques.

Keywords FGM · Stochastic finite element analysis · Shear deformable plate · FORM · SORM

A. Shaker · E. Sadek
Department of Aerospace Engineering,
Cairo University, Cairo, Egypt

W. Abdelrahman
Department of Aerospace Engineering,
King Fahd University of Petroleum and Minerals,
Dhahran 31261, Saudi Arabia

M. Tawfik (✉)
Mechanical Engineering Department,
British University in Egypt, El-Shorouk City,
Cairo 11837, Egypt
e-mail: mohammad.tawfik@bue.edu.eg

1 Introduction

The superior properties of advanced composite materials, such as high specific strength and high specific stiffness, have led to their widespread use in aircrafts, spacecrafts and space structures. In conventional laminated composite structures, orthotropic elastic laminas are bonded together to obtain enhanced mechanical and thermal properties. However, the abrupt changes in material properties across the interface between different materials can result in large interlaminar stresses leading to delamination. Furthermore, large plastic deformations at the interface may trigger the initiation and propagation of cracks in the material. One way to overcome these adverse effects is to use Functionally Graded Materials (FGM), in which material properties vary continuously. This is achieved, for example, by gradually changing the volume fraction of the constituent materials, usually in the thickness direction only, or by changing the chemical structure of a thin polymer sheet to obtain a smooth variation of in-plane material properties and an optimum response to external thermo mechanical loads.

Due to difficulties in tailoring the gradients to actual specifications during manufacturing processes, properties of FGM's are not deterministic in nature. There is a reasonable

body of recent research on studying the effect of uncertainties in material properties on the accuracy of static and thermal analyses of FGM's. In [1], for example, Ferrante and Graham used stochastic simulation to study the effect of microstructural randomness on stress and temperature distributions in FGM's. Later, they added the effect of non-Gaussian porosity randomness on the calculation of thermal distributions [2]. Yang et al. [3] investigated the stochastic bending response of moderately thick FGM plates. In their work they combined a higher order shear deformation plate element and a first order perturbation technique to obtain the second order statistics; mean and variance of the flexural deflection of the plates with various boundary conditions.

Dynamic analysis, however, has not received as much attention, even for the more commonly used laminated composites. In Salim et al. [4] used first order perturbation techniques and FEM formulation to investigate the sensitivity of the natural frequencies of single ply and double ply laminates to randomness of material properties. In Senthil and Batrab [5], obtained exact solutions to the free vibration of FGM rectangular plates. In this work, however, the values of the FGM properties were assumed to be exactly known. Mechanical properties, material density, and plate dimensions, factors that determine the dynamic behavior of FGM plates, are not deterministic in nature. Rather, uncertainties in their values due to manufacturing and fabrication result in variations in the behavior characteristics of the plate such as the values of the natural frequencies. For proper quality control of the dynamic characteristics of laminates, their sensitivities to the laminate properties need to be investigated.

In order to gain knowledge of the sensitivity of the solution to various FGM parameters, a reliability analysis has to be performed. In this work, our previously developed stochastic finite element SFEM analysis of the free vibration of composite laminates [6] is adopted for FGM plates. This analysis allows the random variables representing material properties to be normal or non-normal, correlated or uncorrelated. A choice between the First Order Reliability Method (FORM) and the Second Order Reliability Method (SORM) is facilitated by the procedure. Laminate mechanical behavior is modeled using a higher order shear deformable element. Considerable reduction in calculation time is achieved by deriving the derivatives of the reduced stiffness and mass matrices symbolically. The code is built using the MATLAB 7.1 compiler and all runs are made on a P4 2.8 GHz machine with 512 MB RAM.

2 Stiffness of functionally graded materials

A functionally graded material is often a mixture of two kinds of materials; for example, one can be a metal and the other ceramic. Without losing generality, it can be assumed that the top surface of an FGM plate is ceramic rich and the bottom is metal rich. The region between the two surfaces consists of material blended with both of them, whose distribution is assumed to be in the form of a simple power law [7]:

$$P_e(z) = P_C V_C + P_M (1 - V_C), \tag{1}$$

where P_e, P_C, P_M stand for the effective material properties of the FGM, of the ceramic, and of the metal constituent, respectively. The ceramic volume fraction V_C is a function of the coordinate in the thickness direction, z, and is given by:

$$V_C = \left(0.5 + \frac{z}{h}\right)^n, \quad -h/2 \le z \le h/2, 0 \le n < \infty \tag{2}$$

where h is the plate thickness. $P_e = P_C$, when the exponent $n = 0$, and $P_e = P_M$ as n approaches infinity. The stiffness matrix of a FGM plate, calculated using Eq. (1) is:

$$[Q(z)]_e = [Q]_C V_C + [Q]_M (1 - V_C) \tag{3}$$

where the stiffness matrices of the isotropic constituents are given by:

$$[Q]_{C \text{ or } M} = \begin{bmatrix} Q_1 & Q_{12} & 0 & 0 & 0 \\ Q_{12} & Q_{22} & 0 & 0 & 0 \\ 0 & 0 & Q_{44} & 0 & 0 \\ 0 & 0 & 0 & Q_{55} & 0 \\ 0 & 0 & 0 & 0 & Q_{66} \end{bmatrix}_{C \text{ or } M} \tag{4a}$$

with

$$\left[Q_{11} = Q_{22} = \frac{\mathrm{E}}{1 - \nu^2}, \quad Q_{12} = \nu Q_{11}, \right.$$
$$\left. Q_{44} = Q_{55} = Q_{66} = \frac{E}{2(+\nu)} \right]_{C \text{ or } M}. \tag{4b}$$

3 Reliability models of the composite laminate

Probabilistic analysis can provide necessary information to achieve optimal use of material. The first step in performing such an analysis for the free vibration of a FGM plate, similar to the one in Fig. 1, is to define a suitable and specific performance function. The plate is assumed to be subjected to a

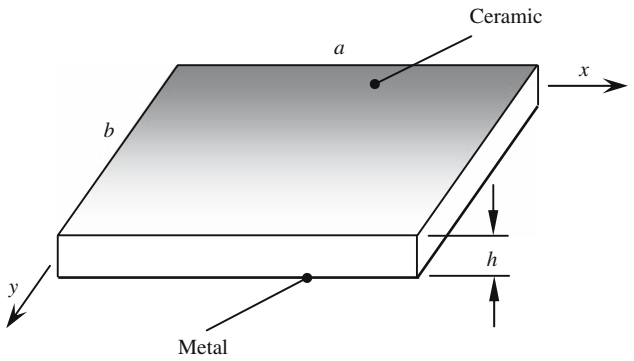

Fig. 1 Geometry of the FGM plate

periodic load with frequency ω_L, which can take any value up to ω_p. This upper limit is not a unique value, but has a certain distribution. This distribution can be quantified by its mean value and standard deviation. At the design point, the plate fundamental frequency ω_p, is equal to a certain specified value ω_r, which may be taken as that of the periodic load. Accordingly, the performance function is defined as:

$$g(X) = (\lambda_p/\lambda_r) - 1 \tag{5}$$

where $\lambda_{p,r} = \omega_{p,r}^2$ are the eigenvalues, and X is a vector of the basic variables. For this plate, X is chosen as:

$$X = [E_C, \nu_C, \rho_C, E_M, \nu_M, \rho_M, n] \tag{6}$$

where ρ_C and ρ_M are the material density of the ceramic and metal, respectively. According to Eq. (5), a failure surface or a limit state of interest can be defined as $g(X) = 0$, with the probability of failure calculated from:

$$p_f = \int \dots \int_{g<0} f_X(X_1, X_2, \dots, X_n) dX_1 dX_2 \dots dX_n, \tag{7}$$

where $f_X(X_1, X_2, \dots, X_n)$, is the joint probability density function for the seven basic random variables. The integration is performed over the failure region $g < 0$. In order to calculate p_f, and following our procedure in [6], we shall use two types of analytical approximations that lead to two methods; the First-Order Reliability Method (FORM-Method 2), and the Second-Order Reliability Method (SORM). Both methods will be investigated in their ability to correctly predict the probability of failure and the Most Probable Point (MPP) of the system. A detailed account of both methods can be found in [8] and will be summarized here.

3.1 First-order reliability method (FORM Method-2)

In this method a Newton-type recursive formula is used to find the design point when the performance function is implicit, as in the case when using finite element formulation to describe the behavior of the system. First the vector X is transformed into a reduced X' with normal random variables of zero mean and unit standard deviation. The starting point of the procedure in the space of X' is usually taken as the point of mean values. This point does not, in general, lie on the limit surface $g(X'_0) = 0$, as shown in Fig. 2 for a two dimensional space. The equation of the limit state is now linearized around X'_0:

$$g(X) = c_0 + \nabla g^T(X'_0) X' \tag{8}$$

Since the performance function is non-linear, then its gradient is not constant. In this case, the new design point is obtained recursively by:

$$X'^*_{k+1} = \frac{1}{\left|\nabla g(X'^*_k)\right|^2} [\nabla g^T(X'^*_k) X'^*_k - g(X'^*_k)] \nabla g(X'^*_k). \tag{9}$$

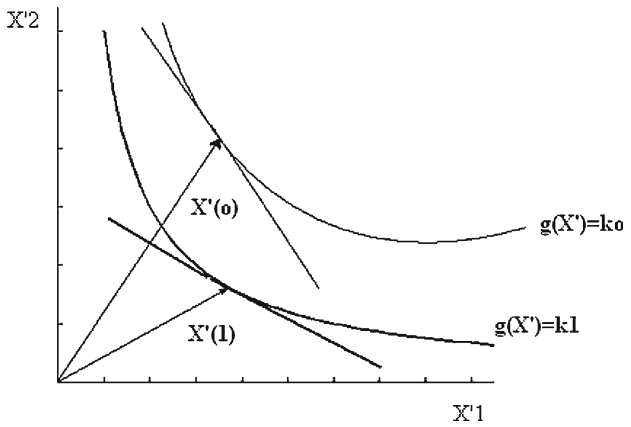

Fig. 2 FORM Method-2 for the non-linear limit state

The distance from the origin to this new design point in the X'-space is:

$$\beta = \sqrt{\sum_{i=1}^{n} X_i'^{*2}}. \tag{10}$$

The procedure is terminated when reaching the most probable point (MPP). MPP is assumed to be reached when both of the following conditions are satisfied:

$$|\beta_{k+1} - \beta_k| \le \varepsilon, \tag{11a}$$

$$\left|g(X'^*_{k+1})\right| \le \delta \tag{11b}$$

with ϵ and δ being reasonably small numbers. The probability of failure in this case is:

$$p_f = 1 - \Phi(\beta), \tag{12}$$

where Φ is the cumulative distribution function of a standard normal distribution with zero mean and unit standard deviation.

3.2 Second-order reliability method (SORM)

This method uses a second order Taylor approximation of the non-linear limit state function in order to better model its curvature. This expansion at a given point X^* in the standard normal variable space is:

$$g(X_1) \cong g(X^*) + \sum_{i=1}^{n} \frac{\partial g}{\partial X_i}(X_i - X_i^*) + \frac{1}{2} \sum_{i=1}^{n} \sum_{j=1}^{n} \left(X_i - X_i^*\right)\left(X_j - X_j^*\right) \frac{\partial^2 g}{\partial X_i \partial X_j}. \tag{13}$$

A simple closed-form solution for the probability of failure using this second-order approximation is derived using

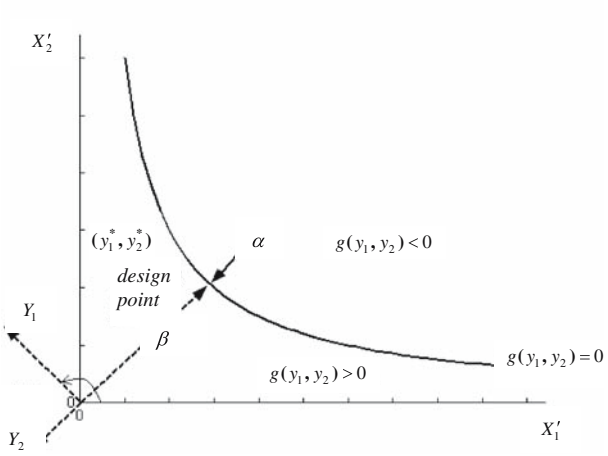

Fig. 3 SORM rotation of coordinates

the theory of asymptotic approximations in as:

$$p_f = \Phi(-\beta) \prod_{i=1}^{n-1} (1 + \beta\kappa_i)^{-0.5}, \tag{14}$$

where β is the reliability index using FORM, and κ_i are the principal curvatures of the limit state at the minimum distance point. These curvatures are obtained as follows. First the X' standard normal variables are rotated to another set of coordinates, denoted as Y, such that the last component of the new set, Y_n, coincides with α, the unit gradient vector of the limit state at the design point. This transformation is shown in Fig. 3 for the case of $n = 2$. This orthogonal transformation is given by:

$$Y = RX' \tag{15}$$

where R is the rotation matrix. For the case $n > 2$, the rows r_i of this matrix are calculated using Gram–Schmidt orthogonalization procedure, see [8], as:

$$r_n = r_{0n}, \tag{16a}$$

$$r_k = r_{0k} - \sum_{j=k+1}^{n} \left[\frac{r_j r_{0k}^T}{r_j r_j^T} r_j \right], \quad k = n-1, n-2, \ldots, 1, \tag{16b}$$

where r_{0i} are the rows of the matrix R_0, given by:

$$R_0 = \begin{bmatrix} 1 & 0 & \cdots & 0 \\ 0 & 1 & \cdots & 0 \\ 0 & \cdots & \cdots & \cdots \\ \alpha_1 & \alpha_2 & \cdots & \alpha_n \end{bmatrix}, \tag{17}$$

with α_ι being the components of the unit gradient vector α at the design point where $i = 1, 2, \ldots, n$.

Defining a matrix A whose elements are denoted by a_{ij} is computed as:

$$a_{ij} = \frac{(RDR^{\mathrm{T}})_{ij}}{|\nabla g(Y^*)|}, \tag{18}$$

where D the $n \times n$ second-derivative matrix of the limit state surface in the standard normal space evaluated at the design point. Since Y_n coincides with the β-vector computed in FORM, the last column and last rows in the A matrix and the last row in the Y vector are dropped out to take this factor into account. The limit state can then be rewritten in terms of a second-order approximation in the rotated Y space as:

$$Y_n = \beta + \frac{1}{2} Y^{\mathrm{T}} A Y, \tag{19}$$

where A is now of size $(n-1) \times (n-1)$. The required curvatures κ_i are computed as the eigenvalues of the matrix A. The probability of failure can now be calculated from Eq. (14).

4 Finite element model

To include transverse shear stresses and rotatory inertia effects into the free vibration analysis of laminates, several shear deformation theories are developed. Here, an element based on the higher-order shear deformation theory (HSDT) is utilized. Development of the element, detailed in [9] and briefly summarized here, employs the parabolic shear deformation theory.

4.1 Displacement field

In the parabolic shear deformation theory, the displacement field is described in terms of midsurface displacements u, v and w, the perpendicular to the midplane, ζ, and the rotations of the normal to the midsurface at $\zeta = 0$, ϕ_1 and ϕ_2. Considering the derivatives of the out-of-plane displacement as separate independent degrees of freedom transforms this system, with 5° of freedom per node and C^1 continuity, into one with 7 degrees of freedom per node and mathematically easier C° continuity. The displacement field may be modified to accommodate C° continuity, see [9]. The resulting displacement field is:

$$\begin{aligned} \bar{u}(x_1, x_2, \zeta, t) &= u + f_1(\zeta)\,\phi_1 + f_2(\zeta)\,\theta_1 \\ \bar{v}(x_1, x_2, \zeta, t) &= v + f_1(\zeta)\,\phi_2 + f_2(\zeta)\,\theta_2 \\ \bar{w}(x_1, x_2, \zeta, t) &= w, \end{aligned} \tag{20}$$

where

$$\theta_1 = \partial w/\partial x_1, \quad \theta_2 = \partial w/\partial x_2, \quad f_1(\zeta) = \zeta - 4\zeta^3/3h^2, \quad \text{and} \quad f_2(\zeta) = -4\zeta^3/3h^2, \tag{21}$$

which satisfies the conditions of stress-free upper and lower plate surfaces.

4.2 Strain energy

The elastic strain energy of the plate as it undergoes deformation is:

$$U = \frac{1}{2}\int_A \bar{\varepsilon}^T D\bar{\varepsilon}\, dA \tag{22}$$

where

$$\bar{\varepsilon} = \left\{\varepsilon_1^0\ \varepsilon_2^0\ \varepsilon_6^0\ \kappa_1^0\ \kappa_2^0\ \kappa_6^0\ \kappa_1^2\ \kappa_1^2\ \kappa_1^2\ \varepsilon_4^0\ \varepsilon_5^0\ \kappa_4^1\ \kappa_5^1\right\}, \tag{23}$$

$$D = \begin{bmatrix} A1 & B1 & E & 0 & 0 \\ B1 & D1 & F1 & 0 & 0 \\ E & F1 & H & 0 & 0 \\ 0 & 0 & 0 & A2 & D2 \\ 0 & 0 & 0 & D2 & F2 \end{bmatrix}, \tag{24}$$

with

$$\left(A1_{ij}, B1_{ij}, D1_{ij}, E_{ij}, F1_{ij}, H_{ij}\right) = \int_{-h/2}^{h/2} Q_{eij}(1, \zeta, \zeta^2, \zeta^3, \zeta^4, \zeta^6)d\zeta, \tag{25a}$$

$$\left(A2_{ij}, D2_{ij}, F2_{ij}\right) = \int_{-h/2}^{h/2} Q_{eij}^{(k)}(1, \zeta^2, \zeta^4)d\zeta, \tag{25b}$$

where i and j take the values 1,2,6 in (25a) and take the values 4,5 in (25b), and components of Q are calculated in Eq. (4).

The strain energy functional is computed for each element and then summed over all the elements in the domain to get the total functional for the domain. Following this procedure, Eq. (22) can be written as:

$$U = \sum_{e=1}^{\mathrm{NE}} U^{(e)} = \sum_{e=1}^{\mathrm{NE}} \frac{1}{2}\int_{A^{(e)}} \bar{\varepsilon}^T D\bar{\varepsilon}\, dA \tag{26}$$

where NE is the number of elements. Upon substituting for the strain vector, the mechanical strain energy becomes:

$$U = q^T K q \tag{27}$$

where K is the global stiffness matrix and q is the global displacement vector.

4.3 Kinetic energy

The kinetic energy of the vibrating plate, within the domain of small displacements, is:

$$T = \frac{1}{2}\int_A \sum_{k=1}^{NL} \int_{-h/2}^{h/2} (\rho \dot{\hat{u}}^T \dot{\hat{u}}\,) d\zeta\, dA, \tag{28}$$

where $\hat{u}$ is the displacement vector given by $\hat{u} = \{\bar{u}\ \bar{v}\ \bar{w}\}$ and ρ is the density calculated using a power law similar to Eq. (1). Similar to the strain energy, this expression can be rewritten as:

$$T = \dot{q}^T M \dot{q}, \tag{29}$$

where M is the global mass matrix.

4.4 FEM formulation

Using variational principles, the governing equations for free vibration for the system can be derived as:

$$Kq + M\ddot{q} = 0. \tag{30}$$

For positive definite M, this equation is transformed into a standard eigenvalue problem:

$$Aq - \lambda q = 0, \tag{31}$$

where $A = M^{-1}K$ and $\lambda_P = \omega_p^2$, with ω_p being the natural frequency of the plate. This FEM formulation, augmented with suitable boundary conditions, is used next to represent the system response when calculating the implicit objective function at each iteration of the stochastic analysis.

5 Stochastic finite element analysis

In reliability analysis, the partial derivatives of the performance function $g(X)$ with respect to all random variables X_i are required. These can be expressed, using the chain rule and Eq. (16) as:

$$\frac{\partial g}{\partial X_i} = \frac{1}{\lambda_r}\frac{\partial \lambda_p}{\partial X_i}, \quad I = 1, 2, \ldots n. \tag{32}$$

The partial derivatives of the jth eigenvalue with respect to the random variables are:

$$\frac{\partial \lambda_j}{\partial X} = \frac{\frac{\partial}{\partial X}\left[\phi_j^T (K - \lambda_j M)\phi_j\right]}{\phi_j^T M \phi_j}, \tag{33}$$

where ϕ_j is the eigenvector corresponding to λ_j.

Noting that K is independent of ρ, while ρ is a common factor of all elements of M, substitution of Eq. (33) into

Eq. (32) yields:

$$\frac{\partial g}{\partial X_i} = \frac{1}{\lambda_r} \frac{\frac{\partial}{\partial X_i}\left[\phi_p^T K \phi_p\right]}{\phi_p^T M \phi_p}, \quad \text{for } i = 1, 2, ..6, 8, 9, \ldots n, \tag{34a}$$

$$\frac{\partial g}{\partial X_7} = \frac{-\lambda_p}{\lambda_r \rho}. \tag{34b}$$

Standard finite difference routines can be used to evaluate the derivatives of the stiffness matrix K in Eq. (34a) with respect to the random variables. This, however, becomes time consuming, especially when the set of random variables include ply orientation angles, because the process is repeated at each iteration point. Moreover, since the prediction of the new point depends on the derivatives, which are approximate in this case, the optimization method takes a larger number of iterations to converge. Finally, using SORM in computing the probability of failure requires calculating the second derivatives as well, which deems the finite difference choice impractical. Use is made of MATLAB symbolic capabilities in evaluating the derivatives of the reduced stiffness and mass matrices. In evaluating the derivative in the numerator of Eq. (34), the eigenvectors at the mean value of X are used, and are not updated at each iteration. This greatly simplifies calculations and is justifiable for large frequency ratios. As the frequency ratio increases, MPP tends to be closer to the mean value of X, which is used in calculating the eigenvectors. Validity of this simplification, and confidence in the whole modeling, is established in our recent work [6] by comparisons with available published results and with results obtained when this simplification is not used.

For the case when all the variables are treated as uncorrelated random variables, the eigenvalue can be assumed to have a statistical distribution with mean and variance calculated at the mean of the random variables, given by:

$$\mu_\lambda \simeq \lambda(\mu_{X_1}, \mu_{X2}, \ldots \mu_{X_n}), \tag{35a}$$

$$\text{Var}(\lambda) = \sigma_\lambda^2 \simeq \sum_{i=1}^{n} \left(\frac{\partial \lambda}{\partial X_i}\right)^2 \text{Var}(X_i). \tag{35b}$$

6 Numerical illustrations

6.1 Full stochastic analysis of a square FGM plate

The first numerical illustration is a simply-supported plate on all edges (SSSS) aluminum-zirconia FGM plate. The plate has a thickness ratio $a/h = 10$. In the present example the ceramic volume fraction exponent is assumed deterministic, $n = 2$. Material properties of the constituents are taken as normal random variables with the distributions shown in Table 1. The tolerances δ and ϵ that determine convergence are taken to be 0.001.

Table 1 Statistical distribution of the basic random variables

Property	E_C (GPa)	E_M (GPa)	ν_C	ν_M	ρ_C (kg/m^3)	ρ_M (kg/m^3)
Mean	151	70	0.3	0.3	3,000	2,707
COV	0.036	0.037	0.0	0.03	0.036	0.036

The calculated non-dimensional natural frequency $\bar{\omega} = \omega a^2 \sqrt{\rho_M / E_M h^2}$ for a 5×5 mesh is 4.7799 which compares very well with the published result of 4.7756 reported in [7]. This latter value was obtained using a 10×10 mesh of quadratic rectangular 8-node serendipity elements.

To the best of our knowledge, full stochastic analyses, with calculated probability of failure, reliability index, and MPP, of the free vibration of FGM plates do not exist in literature. Therefore, the obtained results of the probability of failure will be compared only to those of a developed and verified code in [6] employing Monte Carlo simulation with importance sampling. The aluminium-zirconia plate is analyzed for a frequency ratio FR $= \omega_r/\omega_p = 0.93$. The probability of failure using Monte Carlo simulation technique depends on the number of simulations, as can be seen in Table 2. Therefore p_f can be taken as a dependent random variable, for which one can calculate a mean, a standard deviation and a skewness coefficient. These values for the p_f distribution of Table 2 are 5.362×10^{-5}, 0.01586, −0.00301 respectively. The small value of SD suggests that the value of p_f does not change much around the mean. The negative skewness coefficient means that dispersion is more below the mean than above it. Therefore, taking the mean of Monte Carlo calculated p_f as a reference for comparison is justified and reasonable.

Table 2 shows one of the disadvantages of the use of Monte Carlo simulation to predict the probability of failure for problems with high reliability and relatively low frequency ratios. Since p_f for these cases are very small, convergence is not clearly visible due to round-off error. FORM and SORM algorithms, on the other hand, do not suffer from this problem because convergence is based on the value of β, which for all practical purposes, is a very large number compared to any round-off error. The probability of failure, calculated using FORM, is $p_f = 5.42 \times 10^{-5}$, while that calculated using SORM is $p_f = 5.3625 \times 10^{-5}$. In both methods, the system has to be solved only five times, as compared to the hundreds of times required to get a solution using Monte Carlo simulation, even when importance sampling is used. FORM overestimates the value of the mean of probability of failure by about 1.13%, while SORM overestimates it by only 0.01%. This means that this problem is quasi linear with a small introduced error when the non-linearity is ignored in FORM.

Full stochastic analysis involves determining, not only p_f, but also the MPP and the sensitivity of the performance

Table 2 Variation of p_f of Monte Carlo for SSSS FGM square plate with $a/h = 10$, $n = 2$, and a frequency ratio of 0.93

No. of Simulations	900	1000	1100	1200	1300	1400	1500	1600	1700	1800
$p_f(\times 10^{-5})$	5.04	5.26	5.34	5.46	5.48	5.46	5.41	5.38	5.34	5.45

Table 3 MPP of SSSS FGM square plate with $a/h = 10$, $n = 2$, for three values of the frequency ratio

ω_r/ω_p	E_C (GPa)	E_M (GPa)	ν_C	ν_M	ρ_C (kg/m^3)	ρ_M (kg/m^3)
0.90	137.3	61.3	0.3	0.3	3190.8	3019.1
0.93	141.8	64.2	0.3	0.3	3136.8	2930.8
0.95	144.6	66.0	0.3	0.3	3099.0	2869.0

Table 4 Comparison of the safety index and probability of failure of SSSS FGM square plate with $a/h = 10$, $n = 2$, for three values of the frequency ratio

ω_r/ω_p	FORM		SORM	
	β	p_f	β	p_f
0.90	5.5951	1.10E–8	5.5978	1.09E–8
0.93	3.8710	5.42E–5	3.8737	5.36E–5
0.95	2.7414	3.10E–3	2.7440	3.00E–3

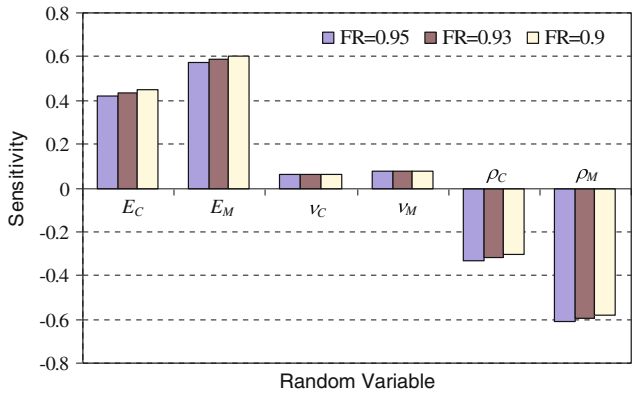

Fig. 4 Sensitivity of g to changes in the random variables for SSSS FGM square plate with $a/h = 10$ and $n = 2$ for different ω_r/ω_p

function to changes in the random variables. Table 3 presents the MPP of the plate for three values of the frequency ratio. It is clear from this table that the variability of the Poisson's ratio of both constituents does not affect the reliability of the solution. Table 4 shows a comparison of the values of the reliability index and the probability of failure, calculated for the three frequency ratios using both FORM and SORM optimization methods.

The sensitivities of the performance function, g, for changes in the random variables are plotted in Fig. 4. The figure shows that, at this particular value of n, with more metal than ceramic, metal properties have a more pronounced

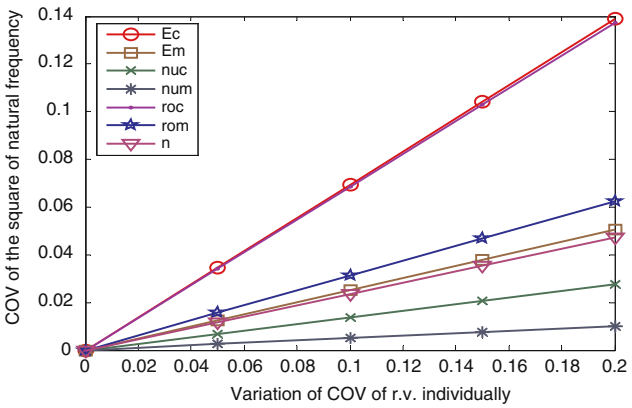

Fig. 5 COV of the fundamental eigenvalue of SSSS FGM square plate with $a/h = 10$ and $n = 0.5$

effect on the solution. The natural frequency is most sensitive to changes in Young's moduli, and is least sensitive to changes in Poisson's ratio, which explains why the values of ν_C and ν_M at the MPP point are almost equal to their mean values. Finally, the figure shows that the relative importance of the variables is the same at all reliability levels of this range. Relative importance can be measured by changes in the COV value of the eigenvalue corresponding to variations in COV of the random variables. This second order statistics investigation is carried out in the second illustration.

6.2 Second order statistics of a square FGM plate

In this example, the variation of the covariance of the square of the natural frequency due to individual variations in the basic random variables is investigated. The FGM plate is the same as that studied in the first illustration. Unlike the first illustration, the randomness of the ceramic volume fraction is considered here. Figs. 5, 6 and 7 show the variation of the COV of the eigenvalue when the COV of each of the random variables varies from 0 to 20%, for $n = 0.5$, 1 and 2, respectively. From these figures it can be concluded that the volume fraction exponent n and the Poisson's ratios ν_M and ν_C have a small effect on the COV of the fundamental eigenvalue, while constituent density and Young's moduli have the most striking effect. This conclusion is even emphasized in Table 5. The table shows the order of importance of the uncertainties on the calculated distribution of λ in a decreasing order of importance for three different compositions of the plate, represented by $n = 0.5$, 1, and 2. It can be seen that

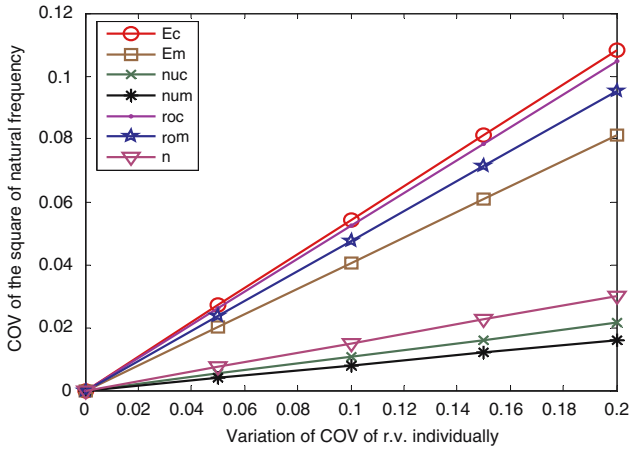

Fig. 6 COV of the fundamental eigenvalue of SSSS FGM square plate with $a/h = 10$ and $n = 1$

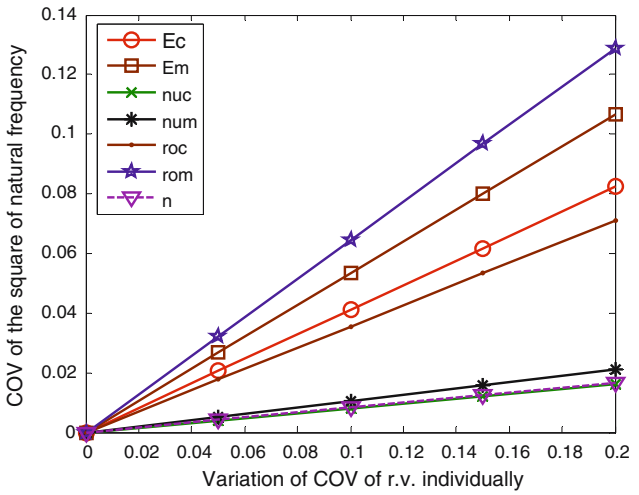

Fig. 7 COV of the fundamental eigenvalue of SSSS FGM square plate with $a/h = 10$ and $n = 2$

Table 5 Order of importance of the random variable uncertainties on λ for SSSS FGM square plate with $a/h = 10$ for three values of $\mu(n)$

$\mu(n)$	E_C	E_M	ν_C	ν_M	ρ_C	ρ_M	n
0.5	1	4	6	7	2	3	5
1.0	1	4	6	7	2	3	5
2.0	3	2	7	5	4	1	6

as n increases, signifying more metal, the plate natural frequency becomes more sensitive to the metal properties than to those of the ceramic.

7 Discussion and conclusions

The potential and versatility of a suggested procedure was demonstrated by applying it to reliability analysis of the free vibration of FGM plates. Using the developed code, the derivative of the performance function with respect to each of the random variables is calculated. These variables included the properties of both constituents and the ceramic volume fraction. FORM and SORM techniques were used to optimize the solution and obtain MPP of the plate. Natural frequency results obtained showed excellent agreement with the limited published results and with Monte Carlo simulation results. FORM Method 2 and SORM were found to be appropriate methods for this problem, and converged after small number of iterations.

The present work lends itself to modifications that add to its speed, accuracy and range of applicable problems. The algorithm can be modified to solve other classes of problems with minor programming modifications and smart choice of the performance function. These include static response, damage characteristics, optimization and forced vibrations.

References

1. Ferrante FJ, Graham L (2001) Randomness effects on the properties of a functionally graded plate using probabilistic methods. In: Structural safety and Reliability: ICOSSAR '01, Newport Beach
2. Ferrante FJ, Graham L (2005) Stochastic simulation of non-gaussian/non-stationary properties in a functionally graded plate. Computer Methods Appl Mech Eng 194:1675–1692
3. Yang J, Liew KM, Kitipornchai S (2005) Stochastic analysis of compositionally graded plates with system randomness under static loading. Int J Mech Sci 47:1519–1541
4. Salim S, Iyengar NGR, Yadav D (1998) Natural frequency characteristics of composite plates with random properties. Struct Eng Mech 6(6):659–671
5. Senthil SV, Batrab RC (2004) Three-Dimensional exact solution for the vibration of functionally graded rectangular plates. J Sound Vib 272:703–730
6. Shaker A, Abdelrahman W, Tawfik M, Sadek E (2008) Stochastic finite element analysis of the free vibration of laminated composite plates. Comput Mech 41:493–501
7. Dai KY, Liu GR, Han X, Lim KM (2005) Thermo-mechanical analysis of functionally graded material (FGM) plates using element-free galerkin method. Comput Struct 83:1487–1502
8. Haldar A, Mahadevan S (2000) Probability, reliability and statistical methods in engineering design. Wiley, New York
9. Shankara CA, Iyengar NGR (1996) AC° Element for the free vibration analysis of laminated composite plates. J Sound Vib 191:721–738